

# THE PHYSICAL REVIEW

*A journal of experimental and theoretical physics established by E. L. Nichols in 1893*

SECOND SERIES, VOL. 77, No. 3

FEBRUARY 1, 1950

## Neutron Diffraction in Liquid Sulfur, Lead, and Bismuth

OWEN CHAMBERLAIN\*

*Department of Physics, University of Chicago, and Argonne National Laboratory, Chicago, Illinois*

(Received September 29, 1949)

A new type of neutron diffraction instrument has been developed to minimize the disadvantage of the broad energy spectrum of available slow neutron sources. It has been used to study the neutron diffraction patterns of the elements sulfur, lead, and bismuth in the liquid state. The patterns have been interpreted in terms of the distribution in separation distance of neighboring pairs of atoms. The results are in reasonable agreement with x-ray diffraction of others. In liquid sulfur each atom has two nearest neighbors at 2.1Å. In liquid lead there are 12 nearest neighbors at 3.4Å. In liquid bismuth an atom has on the average eight neighbors within 4Å, but the nearest neighbors are not well separated from those at greater distance.

### INTRODUCTION

WITH the aid of the relatively large slow neutron flux densities available from piles, it has become possible to use neutron diffraction in the study of the structure of liquids. Presented here are neutron diffraction studies of liquid sulfur, lead, and bismuth, along with a new type of diffraction instrument developed especially to facilitate such studies.

Diffraction studies of liquids with x-rays have been extensive. Following the early work of Hewlett<sup>1</sup> and Keesom and de Smedt,<sup>2</sup> the theoretical analysis of Zernike and Prins<sup>3</sup> gave the detailed connection between the diffraction pattern and the arrangement of molecules within the liquid. The application to liquid mercury by Debye and Menke<sup>4</sup> has been followed by many others. A comprehensive review of x-ray diffraction studies of liquid elements has been given by Gingrich.<sup>5</sup>

The phase and amplitude of slow neutron scattering by various atomic species have been investigated by Fermi and Marshall,<sup>6</sup> using interference effects in solids and gases. Neutron diffraction in polycrystalline

materials has been studied by Wollan and Shull<sup>7</sup> (who give a convenient list of references to earlier papers). Results of these and similar investigations have now been used in the determination of structures of solid matter.<sup>8</sup>

At the present time neutron diffraction studies are more difficult than x-ray diffraction studies for two principal reasons. First, the flux density of slow neutrons available from piles is still much smaller than the effective flux density of x-rays from existing x-ray tubes. By effective flux density of x-rays, we mean the actual flux density of photons times the efficiency for counting with a Geiger counter. It is hoped that higher flux piles may rather soon make neutron diffraction more attractive in this respect. Second, the slow neutrons have a broad energy spectrum (being essentially in thermal equilibrium), whereas much of the intensity from an x-ray tube is concentrated in the characteristic line spectrum of the target material. The design of the instrument used here represents a long step toward the removal of this disadvantage for neutron diffraction.

Neutron diffraction becomes an especially attractive tool in certain special cases in which x-ray diffraction is difficult. Hydrogen, though very difficult to observe in x-ray diffraction, is not much easier to observe in neutron diffraction because a small coherent scattering is masked by a large incoherent scattering. However,

\* Present address: Department of Physics, University of California, Berkeley, California.

<sup>1</sup> C. W. Hewlett, *Phys. Rev.* **19**, 266 (1922).

<sup>2</sup> W. H. Keesom and J. de Smedt, *Proc. Amst. Akad. Sci.* **25**, 118 (1922); **26**, 112 (1923).

<sup>3</sup> F. Zernike and J. Prins, *Zeits. f. Physik* **41**, 184 (1927).

<sup>4</sup> P. Debye and H. Menke, *Physik. Zeits.* **31**, 797 (1930).

<sup>5</sup> N. S. Gingrich, *Rev. Mod. Phys.* **15**, 90 (1943). See also R. Glocker, *Eng. der Exact. Naturw.* **22**, 186 (1949).

<sup>6</sup> E. Fermi and L. Marshall, *Phys. Rev.* **71**, 666 (1947).

<sup>7</sup> E. O. Wollan and C. G. Shull, *Phys. Rev.* **73**, 830 (1948).

<sup>8</sup> Shull, Wollan, Morton, and Davidson, *Phys. Rev.* **73**, 842 (1948).

deuterium gives neutron scattering, mostly coherent, quite comparable to other elements, and offers promise of much information from deuterated hydrogenous substances. Also, some heavy elements have reasonably small neutron capture cross sections, while their x-ray absorption coefficients are uniformly high. Elements of low absorption have been chosen in the present experiments.

Another advantage of the use of neutrons is that the incoherent scattering, which is a perturbing effect and must be subtracted, is under some circumstances large for x-rays and only approximately calculable; it is usually small for neutrons and very nearly spherically symmetric.

The design of the instrument used here is based on the fact (long known in the theory of x-ray diffraction) that the differential scattering cross section of an assembly of atoms is dependent primarily on the magnitude of the change of momentum of the scattered particle or photon. Except for a constant factor, the magnitude of the change of momentum is the same as the scattering parameter  $\sin\theta/\lambda$  commonly used in x-ray diffraction. (Here  $\theta$  is half the angle of deflection of the scattered particle and  $\lambda$  the wave-length.) The present instrument achieves increased intensity over conventional diffraction apparatus by using a fairly wide range of wave-lengths from the incident beam. The angle of deflection  $2\theta$  is a function of the wave-length, such that good resolution in the scattering parameter  $\sin\theta/\lambda$  is obtained.

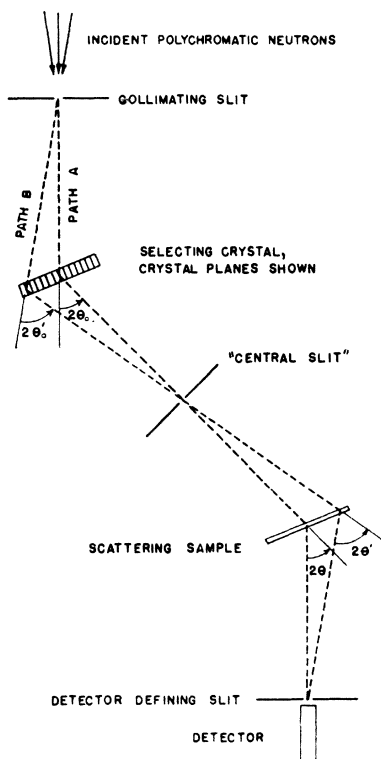


FIG. 1. Schematic diagram of the instrument for the special case

$$\sin\theta/\lambda = 1/2d.$$

The results of the present experiments are to some extent summarized in Figs. 4-6 and 8-11. In liquid sulfur each sulfur atom has two nearest neighbors. In liquid lead each atom has 12 nearest neighbors. In liquid bismuth there is no well-defined group of atoms which can be called nearest neighbors to one atom, but there are eight atoms within a distance of  $4.0\text{\AA}$  from one atom.

#### EXPERIMENTAL ARRANGEMENT

The new diffraction apparatus employed has some similarity to conventional diffraction apparatus, in that Bragg reflection from planes of a single crystal is used to select the proper neutrons from a polychromatic beam. It differs from the conventional apparatus in that the thermal neutron beam incident on the selecting crystal is not a parallel beam but a divergent beam collimated mostly by a single slit. The scattering sample is thin, but of large lateral dimensions. Neither  $\theta$  nor  $\lambda$  separately, but only the quantity  $\sin\theta/\lambda$  is well defined.

It has long been recognized that the factor by which the cross section of a single atom must be multiplied to obtain the cross section for a liquid is a function of  $\sin\theta/\lambda$  only. This fact holds both for x-rays and neutrons; and in the latter case the scattering by a single nucleus is spherically symmetric.

Figure 1 shows a special case in which the angle of deflection at the crystal is equal to the angle of deflection at the scattering sample, so  $\theta_0 = \theta$ . Due to the symmetry around the central slit, this is true for an arbitrary ray through the instrument, i.e.,  $\theta'_0 = \theta'$ . Applying the condition for first-order Bragg reflection  $\lambda = 2d \sin\theta$ ,  $\sin\theta/\lambda = \sin\theta'/\lambda' = 1/2d$ . We describe this fact by saying that for all paths  $\sin\theta/\lambda$  is the same. In a conventional type diffraction apparatus, all usable neutron paths would be very close to the central ray (path A). In this instrument we gain intensity by using other paths as well, such as the path B.

In the limit of a perfect crystal in the form of a thin slab, all neutrons which pass through the first (collimating) slit and are Bragg-reflected will pass through the central slit. There is thus a focusing of the Bragg reflected neutrons here. The existence of this focus point is important to the success of the instrument, for a rather good shield can be placed here to eliminate nearly all but the Bragg reflected neutrons.

Figure 2 shows the apparatus as used for scattering at another (larger) value of  $\sin\theta/\lambda$ . The collimating slit, the selecting crystal, and the first focus slit are unchanged in position, though they are drawn to a more realistic scale. The scattering sample is moved farther from the central slit and its orientation is changed. For neutrons which pass along the central ray of the instrument, we have the Bragg condition for first-order reflection,  $\lambda = 2d \sin\theta_0$ , so

$$\sin\theta/\lambda = (\sin\theta/\sin\theta_0)(1/2d). \quad (1)$$

Neutrons which pass through the instrument along

TABLE I. Spectrometer settings (when Bragg angle at crystal = 15°).

$2\theta$ (counter angle) in degrees	$\frac{\sin\theta}{\lambda}$	$\gamma$	$\varphi$ in degrees
10	0.062	0 (-0.33)	0 (...)
12½	0.077	0 (-0.17)	0 (...)
15	0.093	0	undetermined
17½	0.108	0.18	5
20	0.124	0.35	7½
23½	0.144	0.55	10½
26⅔	0.164	0.80	13
30	0.184	1.00	15
33½	0.204	1.22	16½
36⅔	0.223	1.45	18
40	0.243	1.67	20
43½	0.262	1.89	22½
46⅔	0.281	2.10	26
50	0.300	2.23	30½
53½	0.318	2.33	35
56⅔	0.336	2.37	40
60	0.355	2.38	46
63½	0.373	2.39	51
66⅔	0.390	2.39	55
70	0.407	2.38	58½
73½	0.424	2.33	62
95	0.522	2.33 (...)	62 (...)
117	0.605	2.33 (...)	62 (...)

other rays may be made to have very accurately the same value of  $\sin\theta/\lambda$  because there are two parameters of the instrument which may still be adjusted,  $\varphi$  and  $\gamma$ , defined in Fig. 2. These parameters are adjusted to the two conditions

$$(d\chi/d\alpha)_{\alpha=0} = 0 \quad (2a)$$

and

$$(d^2\chi/d\alpha^2)_{\alpha=0} = 0, \quad (2b)$$

where  $\chi = \sin\theta/\lambda$ .

Since the analytic forms of the expressions in Eqs. (2) are quite cumbersome, these equations are not solved analytically. Instead, a ray-tracing technique is used. The geometry is so adjusted that the central ray and the extreme ray on each side have the same value of the scattering parameter. Through most of the range of the instrument  $\chi$  is then determined to one percent—thus better than the spread due to the slit widths. The values used in setting the apparatus are shown in Table I. Where the calculated values are different from the values used, they are shown in parentheses.

When  $\gamma$  is small, the scattering sample is close to the central slit and  $\varphi$  is essentially undetermined, though the resolution remains good in these cases. When solution of Eqs. (2) gives  $\gamma$  negative, the sample should be on the other side of the central slit—i.e., should have a convergent beam incident upon it. Attempts to realize this situation with cadmium vanes gave poor results due to large backgrounds from scattering off the vanes and incoherent scattering by the selecting crystal. Best practice was found to be to accept slightly poorer resolution by using  $\gamma = 0$ .

The new apparatus described here is useful only when the source has a spectrum wide compared to the

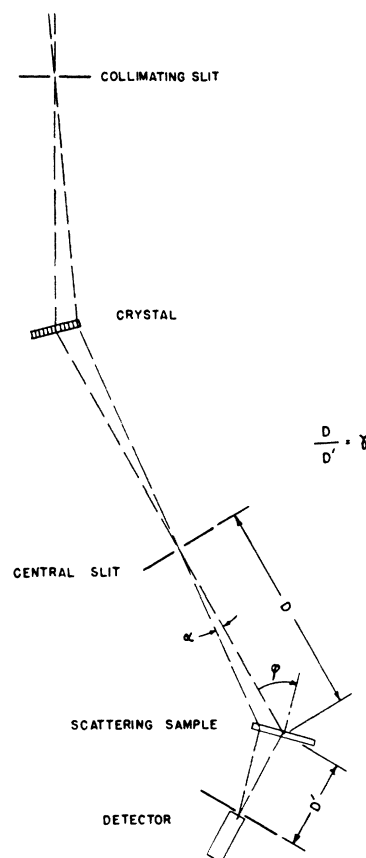


FIG. 2. Schematic diagram showing a typical setting of the instrument.

desired resolution, as the nearly Maxwellian distribution of slow neutrons from a graphite moderator. The apparatus would be useful for x-ray diffraction only in cases where such high resolution was sought that the characteristic x-ray line source appeared broad by comparison.

Figure 3 is a scale drawing of the apparatus. The collimating slit, 2 in. high, ⅞ in. wide, is placed within the shield of the heavy-water pile of the Argonne National Laboratory, at the graphite thermal column. The selecting crystal, placed just outside the shield, is actually four natural crystals of calcium fluoride arranged on a supporting stand for individual adjustment. The single crystals are ½ in. thick. The usable crystal area is 6 by 6 in. in all. The crystals are cut along the natural cube faces and arranged for reflection from the 200 planes. Lower intensity was given by other crystals tried, including natural calcite, artificially crystallized NaCl, PbS, mica (variety unknown), and another natural calcium fluoride crystal.

For the central ray the Bragg angle at the crystal is 15°, this being essentially the largest angle for which second-order reflection is negligible. (Measurement at 21° showed prohibitive (30 percent) second-order content.)

The central slit is 2 in. high, ¾ in. wide, surrounded on all sides by an extensive cadmium shield 0.030 in.

thick. The scattering sample and neutron counter are mounted on a rolling table which can be moved to adjust the distance  $D$ , the motion being parallel to the central ray incident on the scattering sample. The scattering sample can be rotated about a vertical axis and set at will to any desired value of  $\varphi$ . The neutron counter is mounted on an arm for rotation around the same vertical axis on the rolling table, the sample to counter distance  $D'$  being constant.

The usable part of the scattering sample is 6 in. high, 10 in. wide, thickness depending on the scattering material and adjusted for approximately 10 percent scattering in the sample for neutron beam incident normally. Liquid scattering materials are contained in "cells" with thin metal walls. Of several varieties of cell used, only the best will be described. The two sides of large area, through which the beam must pass, are of 0.040-in. aluminum (24S) sheet, welded to an aluminum frame on the side and bottom edges. Supports against

bulging consist of 0.19-inch diameter aluminum rods which penetrate the liquid and are riveted at each end to the 0.040-in. sheet. These rods are placed through the sample on a 2-in. square lattice. Electric heaters are attached at side and bottom edges. Thermal insulation consists of asbestos around the heaters and 0.001-in. aluminum foil over the large sides. The aluminum foil acts as a radiation shield and to enclose a  $\frac{1}{2}$ -in. layer of air around the sample. The greatest temperature difference between two parts of the liquid sample is  $10^{\circ}\text{C}$ .

The scattering by the cell is small (0.015) compared to the scattering by the material within the cell (0.10). Unfortunately, liquid bismuth dissolves some aluminum, approximately one percent by weight (seven percent by number of atoms).

The neutron detector is a pulse ionization chamber with pulse amplifier and scaling circuit. The chamber is of cylindrical construction, outside diameter 2 in., central electrode diameter 0.25 in., active length 8 in., filled with 1 atmos. boron trifluoride enriched in  $\text{B}^{10}$ . Neutrons are incident along the axis of symmetry. The operating voltage is 2000 v and the effective deadtime is  $30 \mu\text{sec}$ . As is to be expected, no true plateau of counting rate *versus* amplifier gain is observed. However, the counting rate is quite insensitive to gain change in the operating region.

Shielding consists mainly of 0.03-in. cadmium sheet or  $1\text{-g}/\text{cm}^2$  boron carbide. Boron carbide is used around all sides of the pulse ion chamber except the front, where a cadmium defining slit is used. The central slit is of cadmium, surrounded by an extensive cadmium shield. Except for the scattering sample, the pulse ion chamber looks only at this cadmium shield. This condition is quite necessary to reduce the background from stray neutrons in the pile room.

For two reasons, the instrument must be calibrated before relative cross sections can be determined. First, the effective counting solid angle of the counter is not strictly a constant because different-sized areas of the scatterer are used at different settings of the instrument. Second, at some settings an additional cadmium diaphragm with fairly large aperture is placed in front of the scattering sample to make absolutely certain that no slow neutrons are scattered by the edges of the sample where there are heaters, supporting frame, etc. Both of these contingencies influence the counting rate in ways not easily calculable.

Calibration is effected by measuring the counting rates of one sample in both a wide beam instrument and a narrow beam instrument. Here the primary apparatus already described is referred to as the "wide beam instrument" whereas "narrow beam instrument" applies to the same apparatus when additional diaphragms with small apertures are added to restrict the beam to a narrow pencil surrounding the central ray. The narrow beam instrument, then, is a conventional diffraction apparatus in which the crystal reflection forms a narrow beam of well-defined wave-length  $\lambda$  and only

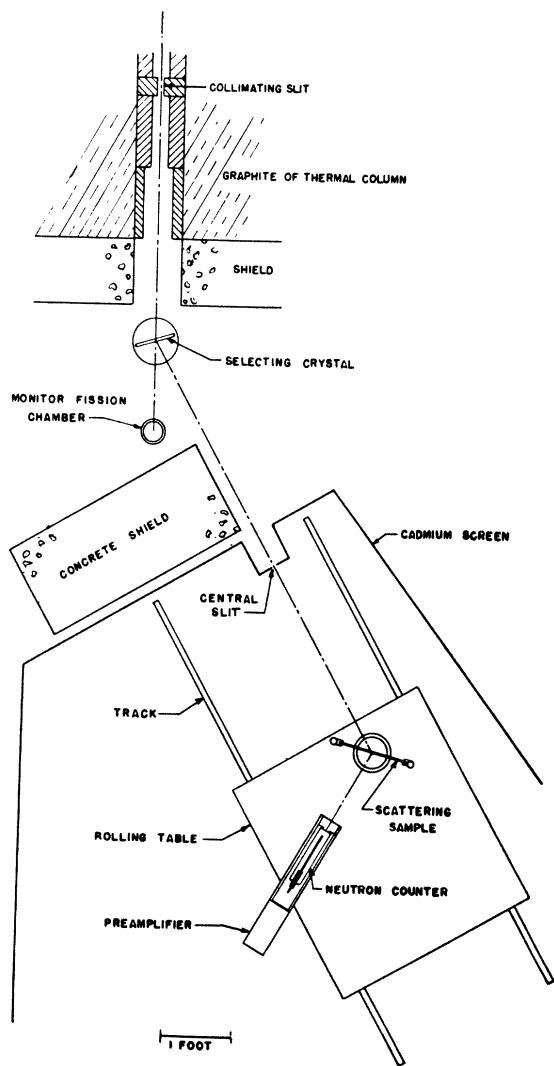


FIG. 3. Plan drawing of the apparatus.

those neutrons count which are deflected through a well-defined angle  $2\theta$  at the scattering sample. Because the narrow beam instrument utilizes only a small area of the scattering sample, results obtained with it are easily interpretable.

In the comparison between narrow and wide beam instruments, a rather thick sample of Plexiglas has been used as scatterer. Its important properties are: (a) It is thick enough (transmission 0.5) to give large scattered intensity and (b) most of the scattering is due to hydrogen, so incoherent scattering predominates and one may be sure the scattering cross section is a slowly varying function of  $\sin\theta/\lambda$ . By using this sample one obtains a counting rate even in the narrow beam instrument sufficient to get good statistical accuracy.

The present instrument is thought to give about six times the intensity of the comparable narrow beam instrument. In instruments of higher resolution, the advantage of the new type instrument should become even greater.

For the determination of the scattered intensity at one angle, counting rates are measured when the sample position is occupied by (a) nothing (except air), (b) an empty cell, (c) an identical cell containing the scattering material (such as liquid sulfur), or (d) a piece of Plexiglas of standard thickness. For each case the counting rate is measured both with and without a cadmium shutter across the central slit. The inclusion of the standard thickness Plexiglas in each run affords some freedom from errors due to slight changes in total neutron flux, changes of the selecting crystal, long term changes in counter efficiency.

The counting rates for a typical sample and average pile level are as follows. Cadmium shutter open: no scatterer, 85 counts/min.; empty cell, 150 counts/min.; full cell (liquid lead), 720 counts/min.; Plexiglas, 2600 counts/min. Cadmium shutter closed; all counting rates between 60 and 120 counts/min. The full cell with shutter open is counted for 8 min., others 4 min. each, which gives the value of the lead scattering relative to the Plexiglass scattering to three percent.

## RESULTS

The direct outcome of the measurements is a determination of the differential scattering cross sections of the materials studied as functions of  $\sin\theta/\lambda$ . More correctly, the differential scattering cross sections relative to the total cross sections are determined. The method of handling the data is outlined in this section.

Fast neutrons, which penetrate cadmium, are eliminated by using only the difference in counting rate, cadmium shutter open and closed. The correction for scattering from air surrounding the sample is accomplished by simple subtraction of the count obtained with nothing in the sample position. (This is adequate since the correction is small.) Correction for the variable solid angle of the counter is accomplished by multi-

plying the counts by the ratio of Plexiglas counts in narrow and wide beam instruments.

Since multiply scattered neutrons contribute a considerable fraction of the counting rate of the full cell, the counting rate is not a strictly linear function of the sample thickness. A correction for multiply scattered neutrons is therefore applied. It is applied separately to full cell and empty cell counting rates.

The counting rate of any sample is considered as

$$S = S' + S'', \quad (3)$$

where  $S'$  is the counting rate due to singly scattered neutrons and  $S''$  is that due to multiply scattered neutrons.  $S'$  contains essentially the scattering in which we are interested.  $S''$  is approximately calculable and is a smoothly varying function of  $\theta$ .  $S''$  averages about 20 percent of  $S'$ .

For the purpose of calculating  $S''$ , the samples are treated as homogeneous—with the material of the cell wall evenly distributed through the sample, and the atoms scattering isotropically. Furthermore, the approximation is used in which the scattered neutrons are considered as originating from the central plane of the sample. We omit details of the calculation.

The properties of the scattering material can conveniently be summarized in the quantity

$$s = [\sigma_T]^{-1}(d\sigma/d\omega). \quad (4)$$

Here  $d\sigma/d\omega$  is the cross section (per atom) for scattering into unit solid angle in a particular direction (the differential scattering cross section) and  $\sigma_T$  is the total cross section (per atom, absorption plus scattering). The relation between  $s$  and the counting rate due to singly scattered neutrons ( $S'$ ) may be given in the form

$$\eta s = (S' \cos\varphi / \Phi\Omega) \{ \eta \sec[2\theta - \varphi] - \eta \sec\varphi / \{ \exp(\eta \sec\varphi) - \exp(\eta \sec[2\theta - \varphi]) \} \}, \quad (5)$$

where  $\eta$  is the negative logarithm of the transmission of the sample,  $\Phi$  is the flux of neutrons through the central slit, and  $\Omega$  is the effective counting solid angle of the neutron counter. From this we calculate the quantity ( $\eta s$ ) for full cell and empty cell.

Denoting the full cell by  $F$ , the empty cell by  $E$ , and the material of interest within the full cell by  $M$ , the scattering properties of  $M$  are obtained from

$$(\eta s)_M = (\eta s)_F - (\eta s)_E \quad (6)$$

and

$$(d\sigma/d\omega)_M = (\eta s)_M / N_M, \quad (7)$$

in which  $N_M$  is the number of atoms per  $\text{cm}^2$  in the sample of scattering material and  $(d\sigma/d\omega)_M$  is the differential scattering cross section per atom for the material of interest.

The differential scattering cross sections for (liquid) sulfur, lead, and bismuth are shown in Figs. 4–6. The observed differential scattering cross section of powdered graphite is shown in Fig. 7, as an indication that the resolution of the instrument is adequate for the present

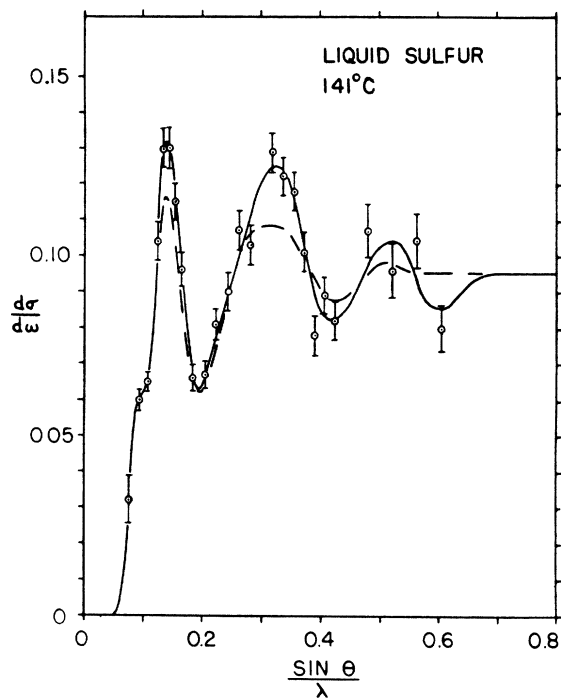


FIG. 4. Differential scattering cross section in barns per steradian as a function of the scattering parameter. The solid curve and the dashed curve show the results of two runs. Experimental points are shown for the solid curve only.

purpose. The observed resolution is in good agreement with that calculated from the geometry of the instrument.

Since the differential scattering cross section is a function only of  $\sin\theta/\lambda$  the (total) scattering cross sections may be calculated. The two runs made with each substance give very closely the same total scattering cross sections. These results are shown in Fig. 8.

#### INTERPRETATION

Attempts to calculate the effects of thermal motion in the liquid on the scattering process have failed. We believe there should occur scattering from aggregates smaller than the typical aggregate involved in the elastic scattering. These scattering events should have a pattern with broader maxima than those of the elastic scattering pattern. In the limit in which one atom scatters independently a completely diffuse pattern will result. Presumably all except the independent scattering from single atoms will be hard to distinguish experimentally from the elastic scattering which already shows broad maxima due to the smallness of the distance over which there is coherence of positions of atoms. We believe these considerations to be in qualitative accord with the scattering phenomena in solids<sup>9</sup> and with a liquid model without potential energy (a closely packed gas of hard spheres).

The average atomic density  $\rho$  at distance  $R$  from any

<sup>9</sup> See W. H. Zachariasen, *Phys. Rev.* **57**, 597 (1940).

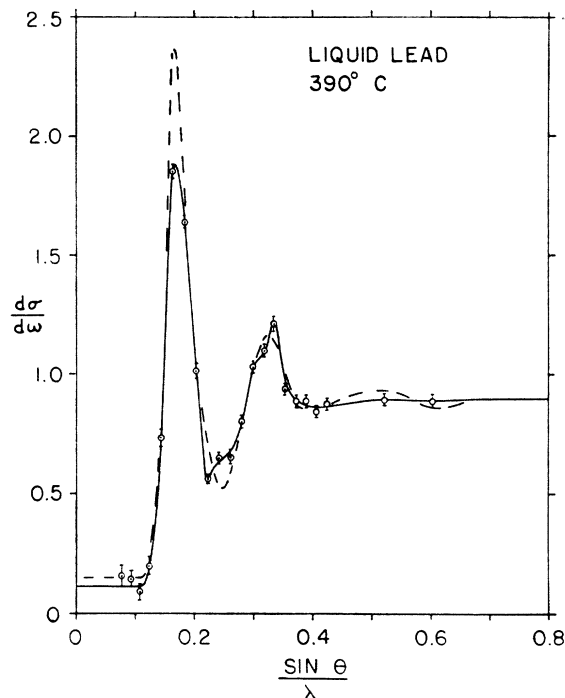


FIG. 5. Differential scattering cross section vs. scattering parameter. Each curve is the result of one run.

atom is calculated by the standard method of Zernike and Prins.<sup>3</sup> This is essentially the Born approximation in which the incident wave at any nucleus is taken as a plane wave to which neighboring nuclei contribute nothing. It may be remarked that coherence of position of atoms in the liquid extends only for a few atomic diameters and the amplitude of the wave scattered by one atom is, at a neighboring nucleus, smaller than the incident wave amplitude by a factor of  $10^4$ . This guarantees the validity of the approximation.

The relation similar to that worked out by Zernike and Prins for x-rays between the distribution function (giving the average atomic density at various distances from one atom) and the differential scattering cross section may easily be derived for the case of neutron diffraction. The differential scattering cross section of an atom for neutrons is a constant independent of angle and nearly independent of wave-length (which is not the case for x-ray scattering). The scattered waves from a group of atoms may be added at great distance from the group. The absolute square of the resultant amplitude gives the scattering cross section for the group which contains a term for each pair of atoms in the group. Since the structure of the liquid is assumed to be repeated many times with random orientation, this is averaged over all orientations of the arrangement. This result depends only on the distance between pairs of atoms in the group. With the introduction of the distribution function, the sum over pairs of atoms may be transformed to an integral. (For details of this

method as applied to x-ray scattering, see Gingrich, reference 5.)

The final result may be written

$$\chi \left( \frac{4\pi}{\sigma_s} \frac{d\sigma}{d\omega} - 1 \right) = \int_0^\infty dR R (\rho - \rho_0) \sin(4\pi\chi R), \quad (8)$$

where  $\chi \equiv \sin\theta/\lambda$ .  $\rho_0$  is the over-all average density of atoms in the liquid,  $\rho$  is the average density of atoms at a distance  $R$  from one atom, and  $\sigma_s$  is the scattering cross section of a (bound) atom. Notice this says that  $\chi[(4\pi/\sigma_s)(d\sigma/d\omega) - 1]$ , which is a function of  $\chi$  only, is essentially the Fourier transform of  $R(\rho(R) - \rho_0)$  which is a function of  $R$ . The conjugate relation is then

$$R(\rho - \rho_0) = 8 \int_0^\infty d\chi \chi \left( \frac{4\pi}{\sigma_s} \frac{d\sigma}{d\omega} - 1 \right) \sin(4\pi\chi R). \quad (9)$$

These relations are derived on the assumption that all atoms of the liquid are identical, and that the spin of the neutron is unaffected in the scattering process. A somewhat more general derivation may take account of isotope and spin effects. The resulting relations are the same as those above, with the coherent scattering cross sections in place of total scattering cross sections.

Coherent differential scattering cross sections are obtained here by subtraction of the observed incoherent scattering from the total scattering. The incoherent cross section is taken to be that observed at very small angles, since the incoherent scattering is (very nearly)

isotropic. In the present experiment slightly more incoherent scattering is observed in liquid lead and liquid bismuth than that reported by Fermi and Marshall in solid samples, presumably due to a small second-order content of the Bragg reflected beam used in the present experiment. Second-order reflection in the crystal gives scattered intensity at half the proper value of  $\sin\theta/\lambda$ . The difference in incoherent scattering observed here and that reported by Fermi and Marshall is considered negligible, both from the standpoint of experimental result and from the standpoint of the effect on the calculated distribution in  $R$ . In liquid sulfur the incoherent scattering could not be determined because measurements could not be made at sufficiently small values of  $\sin\theta/\lambda$ . No correction for incoherent scattering was made in this case.

Before proceeding with the Fourier analysis for the distribution in  $R$ , it is important to be sure of the normalization of the results for  $(d\sigma/d\omega)/\sigma_s$ . This quantity, if calculated directly, depends upon the factor  $\sigma_T/\sigma_s \eta \Phi \Omega$ , in which neither  $\eta$  nor  $\Phi \Omega$  are known as accurately as the counting rates. An alternative procedure is used to establish proper normalization of  $d\sigma/d\omega$ , similar to the method common in x-ray diffraction. It is assumed that the density of atoms at distance  $R$  from one atom approaches zero as  $R$  approaches zero. The relations of Zernike and Prins then guarantee that

$$\int_0^\infty d\chi \chi^2 \left( \frac{4\pi}{\sigma_s} \frac{d\sigma}{d\omega} - 1 \right) = -\frac{\rho_0}{32\pi}, \quad (10)$$

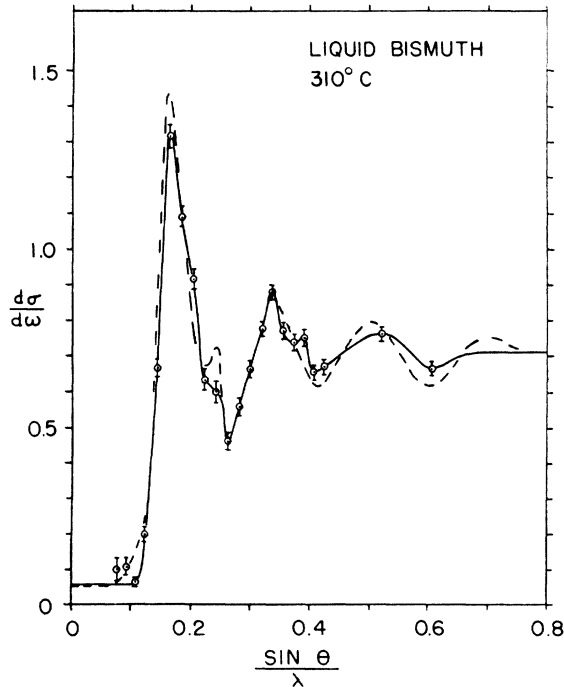


FIG. 6. Differential scattering cross section vs. scattering parameter. Each curve is the result of one run.

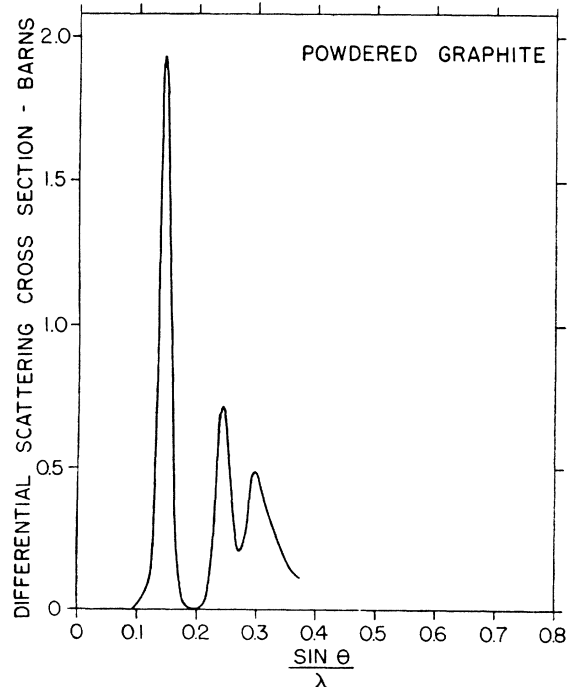


FIG. 7. Apparent differential scattering cross section of powdered graphite, used to indicate the resolution of the instrument.

where  $\rho_0$  is the average numerical atomic density. Use of this relation establishes the normalization. It may be remarked that the less accurate but more straightforward normalization using  $\eta$  and  $\Phi\Omega$  gives the same results to within a few percent.

Evaluation of the Fourier transform and hence of  $\rho(R)$  is accomplished by the method of trigonometric interpolation, described in detail by Danielson and Lanczos.<sup>10</sup> Curves are drawn of the coherent differential scattering cross section *vs.*  $\chi$  from which 32 values equally spaced (in  $\chi$ ) are taken. From these 32 points an equal number of values of the Fourier transform are obtained. Since it is difficult to specify the probable error of the values of the Fourier transform, the data for each material are divided into two groups corresponding to two runs and  $\rho(R)$  separately evaluated. Only those features which both determinations have in common may be considered significant.

Results are shown in Figs. 9–11. The ordinate is  $4\pi R^2\rho$ ; the abscissa is  $R$ , the distance from one atom. Also shown for comparison is  $4\pi R^2\rho_0$ .

Figure 9 for liquid sulfur requires special comment in that in one run the differential scattering cross section was not extended as far to large values of  $\chi$  as the other. As a result, this run (shown with crosses in Fig. 9) gives poorer resolution in  $R$ , and less definite deviations from the curve representing the average density. The

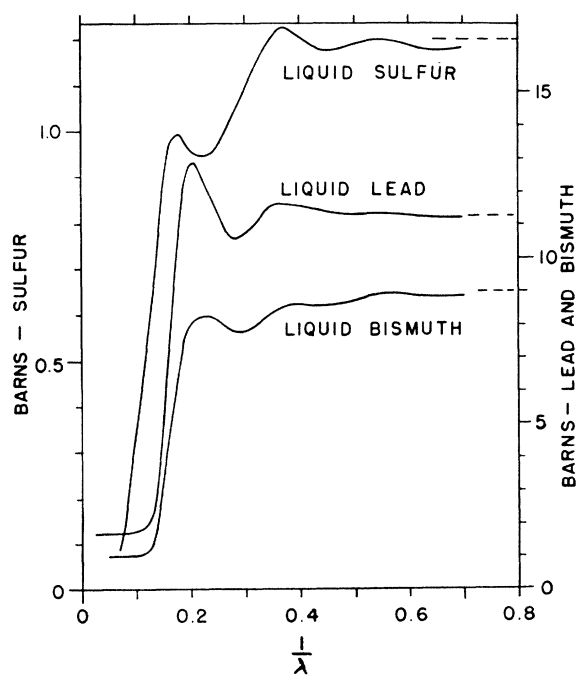


FIG. 8. Total scattering cross sections as functions of the inverse wave-length.

<sup>10</sup> G. C. Danielson and C. Lanczos, *J. Franklin Inst.* **233**, 365 (1942); **233**, 435 (1942).

other curve (shown with circles) should be given greater weight, and agrees well with results of Gingrich.<sup>11</sup> Each atom has two nearest neighbors at about 2.1Å with few or no other atoms at 2.6Å. The density is greater than average from 4Å to 5Å and slightly less than average at 6Å from one atom. This distribution function is consistent with, but does not prove, the existence of closed chains of eight atoms.

Figure 10 is a similar plot for liquid lead. The first maximum at 3.4Å represents  $12(\pm 1)$  nearest neighbors, not completely separated from other lead atoms. The curve shows a deficiency of atoms at 4.7Å and 8Å and an excess at 6.4Å. Glocker and Hendus,<sup>12</sup> who have studied the x-ray diffraction of liquid lead, find eight neighbors with four more only slightly farther away. Only if the data were extended to much larger values of  $\chi$ , could the present work be expected to resolve the two groups. Otherwise, the agreement with Glocker and Hendus is very close. Although the distribution function does not fit easily any picture of a loosely packed but solid-like structure, the hexagonal close-packed structure comes closest of any to fitting the observed distribution for lead.

Figure 11 shows the same data for liquid bismuth. In bismuth it is hard to count the nearest neighbors because they are not readily distinguishable from the atoms at greater distance. To 4Å there are eight atoms. Significant excesses are found at 3.2Å and 6.7Å, and

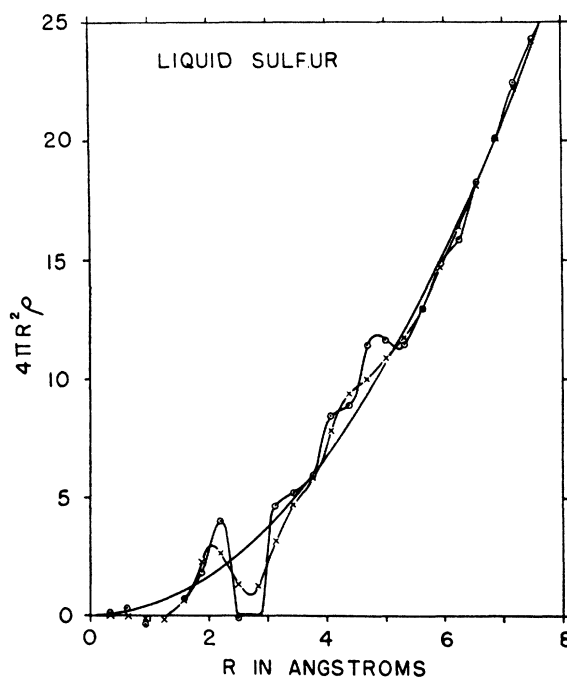


FIG. 9. The number of atoms per unit distance from one atom as a function of the distance. Results from two runs are shown.

<sup>11</sup> N. S. Gingrich, *J. Chem. Phys.* **8**, 29 (1940).

<sup>12</sup> R. Glocker and H. Hendus, *Ann. d. Physik* **43**, 513 (1943).

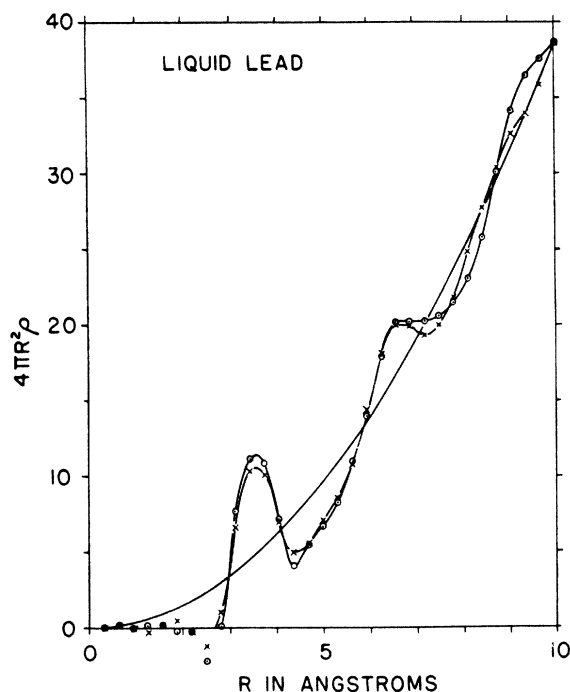


FIG. 10. The number of atoms per unit distance from one atom as a function of the distance. Results from two runs are shown.

deficiencies at 5.3Å and 7.7Å.† The liquid bismuth structure shows little similarity to simple solid structures.

The variation with energy of the total cross section of liquid lead given here may be compared with that given by Havens, Rabi, and Rainwater.<sup>13</sup> The results given here show less decrease in cross section with increasing wave-length, however, the error in the

† *Note added in proof:* The data of Fig. 11 are in close agreement with those of Hendus who has studied liquid bismuth using x-ray diffraction; H. Hendus, *Zeits. f. Naturforschung* **2A**, 505 (1947).

<sup>13</sup> Havens, Rabi, and Rainwater, *Phys. Rev.* **72**, 634 (1947).

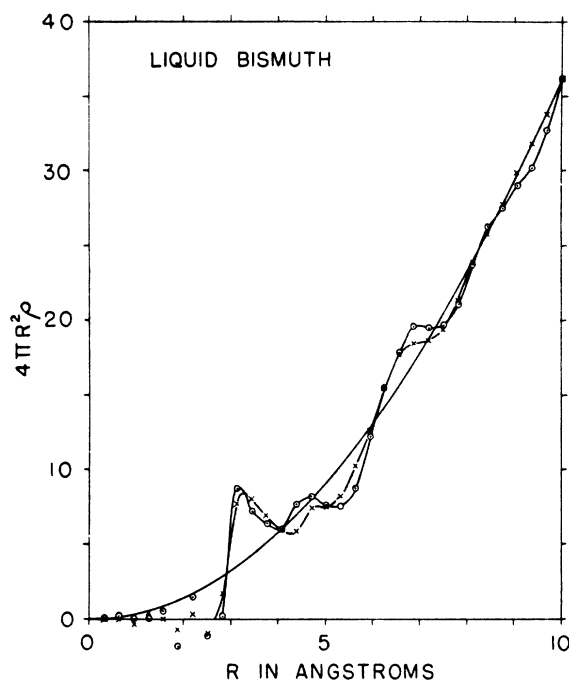


FIG. 11. The number of atoms per unit distance from one atom as a function of the distance. Results from two runs are shown.

present result does not preclude the energy dependence given by Havens, Rabi, and Rainwater. One can only say that the two results are consistent.

The author wishes to express his gratitude to Professor E. Fermi for suggesting this subject for study and for advice during the investigation. Dr. A. Wattenberg of the Argonne National Laboratory has been of great assistance in making suggestions, in making available to him much of the equipment used, and in taking some of the data. The very essential aluminum fabrication and much of the construction of the instrument has been done by Mr. J. Dalman of the Argonne National Laboratory Staff.